

Electronic coherence in metals: Comparing weak localization and time-dependent conductance fluctuations

A. Trionfi, S. Lee, and D. Natelson

Department of Physics and Astronomy, Rice University, 6100 Main Street, Houston, Texas 77005, USA

(Received 7 May 2004; published 14 July 2004)

Quantum corrections to the conductivity allow experimental assessment of electronic coherence in metals. We consider whether independent measurements of different corrections are quantitatively consistent, particularly in systems with spin-orbit or magnetic impurity scattering. We report weak localization and time-dependent universal conductance fluctuation data in quasi-one- and two-dimensional AuPd wires between 2 and 20 K. The data inferred from both methods are in excellent quantitative agreement, implying that precisely the same coherence length is relevant to both corrections.

DOI: 10.1103/PhysRevB.70.041304

PACS number(s): 73.23.-b, 72.70.+m, 73.20.Fz, 73.50.-h

Quantum coherence of electrons in solids remains a topic of much interest. Technologically, coherent control and manipulation of electrons is relevant in proposed novel devices.^{1,2} Scientifically, the mechanisms and temperature dependence of decoherence are of fundamental importance,³ and have profound implications for the ground state of metals in the presence of disorder. Quantum corrections to the conductivity allow coherence to be examined experimentally. Specific corrections that have been used include the weak localization (WL) magnetoresistance,⁴ universal conductance fluctuations as a function of magnetic field^{5,6} (MFUCF), time-dependent universal conductance fluctuations (TDUCF),^{7,8} and Aharonov-Bohm oscillations.⁹

These corrections result from interference between electronic trajectories on length scales shorter than the coherence length, $L_\phi \equiv \sqrt{D\tau_\phi}$, where D is the electron diffusion constant and τ_ϕ is the time scale over which the phase of the electron's wave function is perturbed strongly by environmental degrees of freedom. It is interesting to ask whether precisely the same time (length) scales are relevant to the various quantum corrections. For example, the electron "out-scattering" time (for scattering out of a particular momentum state) in the Boltzmann equation with screened Coulomb interactions has a different temperature dependence¹⁰ than the coherence time for weak localization,^{3,11} and has been suggested as relevant to UCF.¹² One must also consider whether other complications (e.g., spin-orbit coupling; scattering from dilute magnetic impurities) affect the inferred values of L_ϕ identically. Subtleties are known to exist regarding magnetic impurities in Aharonov-Bohm rings.¹³ These questions have particular relevance as recent publications concerning saturation¹⁴ of $L_\phi^{\text{WL}}(T)$ as $T \rightarrow 0$ have included comparisons with Aharonov-Bohm experiments¹⁵ and MFUCF data.¹⁶

Weak localization results from electron trajectories that form closed loops, and their time-reversed conjugates. With no spin-orbit scattering and at zero magnetic field, such pairs constructively interfere, leading to a lowered conductance. Strong spin-orbit interactions lead instead to destructive interference, and a conductance increase at zero magnetic field. Magnetic flux through such a loop suppresses these interference effects, resulting in a magnetoresistance with a field scale that reflects L_ϕ^{WL} and the sample geometry.

Time-dependent UCF result from changes in defects' positions that alter the phases of interfering trajectories, and hence the conductance within a coherent volume. With an appropriate broad distribution of defect relaxation times, the resulting noise power has a $1/f$ dependence.¹⁷ Applied magnetic flux suppresses the cooperon contribution to the fluctuations¹⁹ over a field scale related to L_ϕ^{TDUCF} , reducing the noise power by a factor of two. As $T \rightarrow 0$, L_ϕ^{TDUCF} grows relative to sample size, L , and thermal smearing is reduced, leading to an increase of TDUCF noise power. For WL and the field dependence of TDUCF,¹⁸⁻²⁰ the quasi-1D limit occurs in samples of width w and thickness t when $w, t < L_\phi$, while the quasi-2D limit occurs when $t < L_\phi < w$. The thermal length, L_T , is defined as $L_T \equiv \sqrt{\hbar D/k_B T}$ and is important for determining the magnitude of UCF.

Previous experimental comparisons between L_ϕ^{WL} and L_ϕ^{TDUCF} were equivocal. In quasi-2D silver films,^{21,22} the two lengths agreed quantitatively only above a temperature where $L_\phi^{\text{TDUCF}} \approx L_{\text{SO}}$, the spin-orbit scattering length. At 2 K, $L_\phi^{\text{WL}} \sim 2 \times L_\phi^{\text{TDUCF}}$. The results were interpreted as consistent with L_ϕ^{WL} set by Nyquist scattering and L_ϕ^{UCF} determined by the out-scattering rate.¹² Similar investigations in quasi-1D Li wires²⁰ showed better agreement between L_ϕ^{WL} and L_ϕ^{TDUCF} in a weak spin-orbit system, but data were limited. A theoretical reexamination²³ now predicts agreement between these lengths in both quasi-1D and quasi-2D systems when decoherence arises from electron-electron interactions. This agreement is expected to remain true²⁴ as long as other decoherence mechanisms (e.g., electron-phonon; spin-flip scattering) do not involve small ($\ll k_B T$) energy transfers.²³

We compare L_ϕ^{WL} and L_ϕ^{TDUCF} in mesoscopic AuPd wires in both the quasi-1D and 2D limits. The AuPd is known to have extremely strong spin-orbit scattering.²⁵ One quasi-2D sample was deliberately contaminated with ferromagnetic impurities. We find that coherence lengths inferred from both WL and TDUCF are in strong numerical agreement between 2 and 20 K, independent of dimensionality and magnetic impurity concentration. This agreement implies that coherence lengths inferred from these different experimental techniques may be compared *quantitatively*, even in the presence of significant spin-orbit interactions and decoherence due to spin-flip scattering.

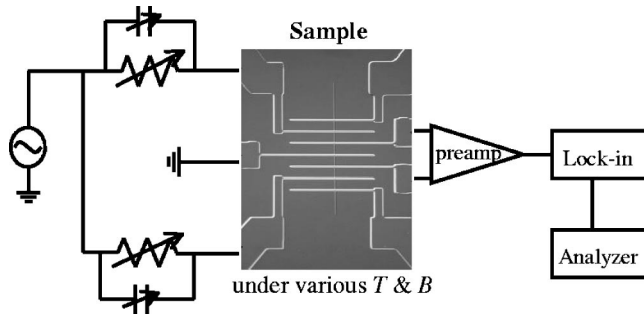


FIG. 1. Noise measurement scheme. Trimming capacitors are used to null away any capacitive phase differences between the two bridge halves. The samples consist of seven leads with only five consecutive leads used.

All samples were fabricated by electron beam lithography on undoped GaAs substrates. Figure 1 shows the sample configuration, and the parameters for each sample are described in Table I. For each sample between 6.5 and 9 nm of $\text{Au}_{0.6}\text{Pd}_{0.4}$ was evaporated to create the wire, followed by a second lithography step to create the leads. The leads consisted of 1.5 nm thick Ti and followed by 25 nm of Au. Each segment of wire between Ti/Au leads was 10 μm in length, and each wire consisted of seven segments. All evaporations were performed via an electron beam evaporator at $\sim 5 \times 10^{-7}$ millibars. Knowing the purity of the starting material, the AuPd alloy likely contains magnetic impurities at the few parts per million level, as discussed below. To produce a sample (D) with a higher magnetic impurity concentration, roughly 2.5 nm of $\text{Ni}_{0.8}\text{Fe}_{0.2}$ was evaporated with the sample shutter *closed* immediately prior to AuPd deposition. Contact resistances were less than 30 Ω . Diffusion constants were calculated using the Einstein relation and the density of states for bulk Au.²⁶

Samples were measured in a ^4He cryostat and initially characterized by four-terminal resistance versus temperature in a 3 T magnetic field normal to the wire. Magnetic impurity concentrations in all samples were sufficiently low that no Kondo upturn in resistivity was distinguishable. Currents from 10 nA to 10 μA were set at each temperature such that no Joule heating was detected in $R(T)$.

All noise measurements were performed using a five-terminal ac bridge technique²⁷ with a carrier frequency of 600 Hz. No drive current dependence was observed in either WL or TDUCF until currents large enough to affect $R(T)$. WL magnetoresistance was measured in a four-terminal con-

TABLE I. Samples used in magnetotransport and noise measurements. Free electron density of states for Au used to calculate D : $1 \times 10^{47} \text{ m}^{-3} \text{ J}^{-1}$, from Ref. 26. Sample D was deliberately contaminated with additional ferromagnetic impurities.

Sample	w [nm]	t [nm]	R_{\square} [Ω]	D [m^2/s]
A	43	9	32.1	1.34×10^{-3}
B	35	9	31.5	1.34×10^{-3}
C	500	6.5	84.5	7.9×10^{-4}
D	500	8.5	47.9	9.6×10^{-4}

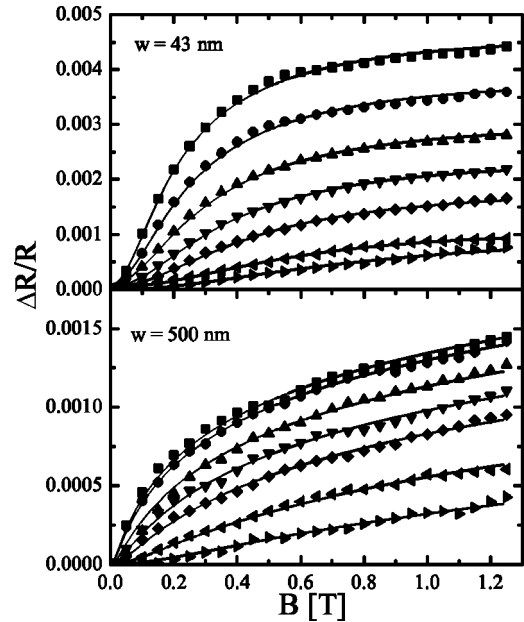


FIG. 2. Weak (anti)localization magnetoresistance at various temperatures for a 43 nm wide wire (quasi-1D, top) and a 500 nm wide wire (quasi-2D, bottom), with fits to Eqs. (1) and (2) respectively. Top to bottom, temperatures are 2 K, 4 K, 6 K, 8 K, 10 K, 14 K, and 20 K.

figuration while varying a perpendicular magnetic field between ± 1.25 T. For the TDUCF, the demodulated lock-in output was fed into a dual channel signal analyzer to transform the signal into the frequency domain. A typical frequency range was 78 mHz to 1.5 Hz. Background pre-amp noise was measured simultaneously using the out-of-phase output of the lock-in, and subtracted from the in-phase noise signal. Excellent agreement with a $1/f$ dependence of the noise power was found consistently. As expected for TDUCF, the measured noise power increased as $T \rightarrow 0$, and depended nontrivially on B as described below.

Figure 2 shows typical magnetoresistance curves for a quasi-1D and a quasi-2D sample. The WL magnetoresistance formulas with strong spin-orbit interactions for 1D and 2D are

$$\left. \frac{\Delta R}{R} \right|_{1\text{D}} = -\frac{e^2}{2\pi\hbar} \frac{R}{L} \left[\frac{1}{L_{\phi}^2} + \frac{1}{12} \left(\frac{w}{L_B} \right)^2 \right]^{-1/2}, \quad (1)$$

$$\left. \frac{\Delta R}{R} \right|_{2\text{D}} = \frac{e^2}{4\pi^2\hbar} R_{\square} \left[\psi \left(\frac{1}{2} + \frac{1}{2} \frac{L_B^2}{L_{\phi}^2} \right) - \ln \left(\frac{1}{2} \frac{L_B^2}{L_{\phi}^2} \right) \right], \quad (2)$$

respectively.^{25,28} The differing forms result from divergences that depend on dimensionality.²⁹ Note that $\Delta R = R(B) - R(B = \infty)$ for Eq. (1) while $\Delta R = R(B) - R(B = 0)$ for Eq. (2). Here ψ is the digamma function, L_B is the magnetic length and is defined as $L_B \equiv \sqrt{\hbar/2eB}$, and R_{\square} is the sheet resistance. In fitting the quasi-1D magnetoresistance data, at 2 K the width w was allowed to vary, and was then fixed for all other fits. Widths found in this manner (43 nm and 35 nm) were consistent with both electron micrographs and estimates based on measured resistances and R_{\square} found in codeposited films.

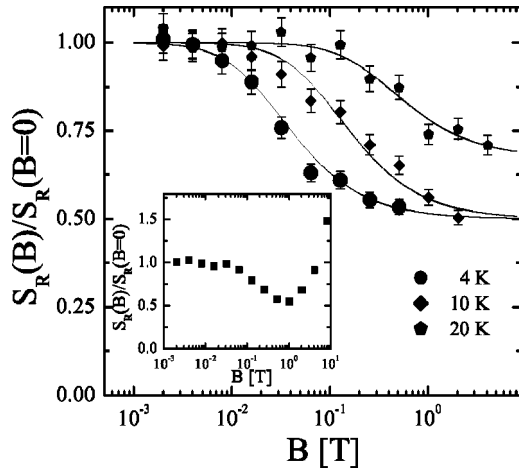


FIG. 3. Normalized noise power as a function of magnetic field for a 500 nm wide wire. The 20 K point does not drop by a full factor of 2 due to local interference noise. Inset: At high field there is a large upturn in the noise for a sample deliberately dosed with additional magnetic impurities (500 nm wide sample at 4 K).

Including L_{SO} as a fit parameter leads to $L_{SO} \lesssim 10$ nm, with little impact on L_ϕ .

Figure 3 shows examples of the normalized noise power ($S_R(B)/S_R(B=0)$) as a function of field. As in WL, the characteristic field scale involves magnetic flux through loop-like trajectories, with a lower field corresponding to a larger L_ϕ^{TDUCF} . The normalized noise power as a function of B is the crossover function, $\nu(B)$, and depends on dimensionality. Analytical expressions for the crossover functions in the strong spin-orbit limit have recently been calculated:²⁴

$$\nu_{1D}(B) = 1 - \frac{x}{2} \left(\frac{\text{Ai}(x)}{\text{Ai}'(x)} \right)^2, \quad (3)$$

where $x \equiv L_\phi^2 / (3(\hbar/Bew)^2)$, and

$$\nu_{2D}(B) = \frac{1}{2} + \frac{L_B^2}{4L_\phi^2} \psi' \left(\frac{1}{2} + \frac{L_B^2}{2L_\phi^2} \right), \quad (4)$$

respectively. These functional forms are strictly valid when $\hbar/\tau_\phi \ll k_B T$. Here $\text{Ai}(x)$ is the Airy function, and $\psi'(x)$ is the derivative of the digamma function.

Previous L_ϕ^{TDUCF} extractions^{20–22} have used the numerical crossover function calculated by Stone¹⁹ for quasi-2D samples, as well as an approximate analytical form derived by Beenakker and van Houten³⁰ for 1D samples. Comparisons between the analytic and numerical forms demonstrated T -independent differences (numerical > analytical) of roughly 14% for quasi-1D samples and 3% for quasi-2D samples. As in the WL data, the resulting fits were essentially unaffected by including L_{SO} as a fit parameter, since L_{SO} is so short.

To account for field-independent local interference noise^{31,32} at higher temperatures, a second fitting parameter, z , the fraction of noise that is due to UCF, was introduced into the fitting function, $f(B) = (1-z) + z\nu(B)$. We found that z was indistinguishable from 1 for all temperatures measured except for 20 K in the 2D samples, when $z \approx 0.68$. All fits

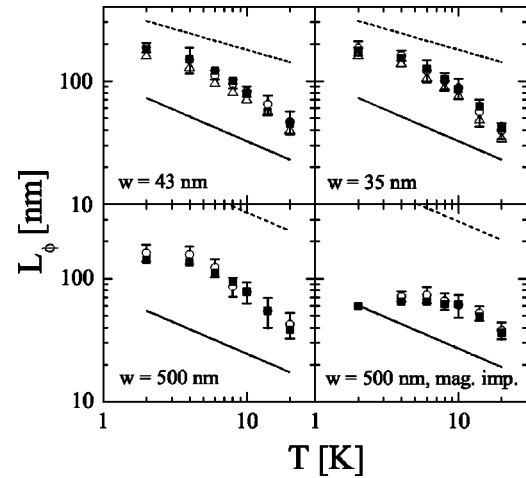


FIG. 4. The coherence lengths of the four samples, as indicated. Closed squares: WL data; open circles: Beenakker/van Houten/Stone (Refs. 19 and 30) fit to TDUCF field dependence; open triangles: Aleiner fit [Eq. (3)] to TDUCF field dependence. Only one TDUCF fit is shown for the 2D samples since both fits result in the same number to within 3%. Dashed lines are predicted values for L_ϕ assuming decoherence is dominated by Nyquist scattering (Ref. 33) and using sample parameters from Table I. Solid lines are L_T values calculated from the same sample parameters.

and confidence intervals were determined by nonlinear χ^2 minimization and analysis.

The inset to Fig. 3 shows the normalized noise power as a function of field for the magnetically contaminated sample. The upturn at large fields is a suppression of spin-flip decoherence as the Zeeman splitting of the magnetic impurities exceeds $k_B T$. An analogous upturn has been observed in investigations of Li wires²⁰ and in recent Aharonov-Bohm measurements in Cu rings.¹⁵ Some upturn is visible at the highest B/T ratio in *all* of our samples, consistent with some magnetic impurities even in nominally “clean” devices. Note that the effects of spin-flips on WL and TDUCF depend on the ratio of the spin-flip time and the temperature-dependent impurity Korringa time.²⁸ For $T > \sim 40$ mK \times the ppm concentration of magnetic impurities, spin-flip scattering should involve large energy transfers,²⁴ and affect WL and TDUCF identically. For our samples (with \sim a few ppm impurities), this crossover is well below 1 K, outside the regime of these experiments.

The resulting coherence lengths from both WL and UCF measurements are shown in Fig. 4. The temperature dependence becomes steeper as electron-phonon scattering increases. Clearly, over the temperature range measured the coherence lengths inferred from the two techniques are in excellent agreement. This agreement remains strong even in the presence of magnetic impurity scattering significant enough to suppress the coherence length by more than a factor of two. This strongly supports the theoretical statement²³ that weak localization and UCF measurements probe *precisely* the same coherence physics, even in the presence of strong spin-orbit and magnetic impurity scattering.

The agreement is noteworthy. First, L_ϕ values at the lowest temperatures are below those predicted from the pure Nyquist electron-electron dephasing (for example, see Ref.

33). This is not surprising given the presence of magnetic impurities in the AuPd, as described above. Second, the agreement persists even though \hbar/τ_ϕ is never $\ll k_B T$, suggesting that Eqs. (3) and (4) are robust even when that constraint is somewhat relaxed.

These results leave open the question of why the coherence lengths in Ag inferred from WL and TDUCF have differing temperature dependencies.^{21,22} The simplest explanation would involve some subtle effect from triplet channel interactions that is only relevant when $L_{SO} \sim L_\phi$. Until further theoretical and experimental investigations address this regime, any quantitative attempts to compare different coherence phenomena in materials with intermediate spin-orbit scattering should be done with care.

We have carefully measured weak localization magnetoresistance and the magnetic field dependence of time-dependent universal conductance fluctuations in mesoscopic AuPd wires. By comparing the coherence lengths inferred from these data, we have shown that L_ϕ^{WL} and L_ϕ^{TDUCF} are in quantitative agreement, even in the presence of potentially subtle effects such as strong spin-orbit scattering and spin-flip contributions to dephasing. Numerical consistency should therefore be expected between complementary UCF and WL measurements of electronic coherence.

We would like to thank N. O. Birge for his helpful advice concerning noise measurements, and I. L. Aleiner and A. D. Stone for discussions of the theory. This work was supported by DOE Grant No. DE-FG03-01ER45946/A001.

-
- ¹W.J. Liang, M. Bockrath, D. Bozovic, J.H. Hafner, M. Tinkham, and H. Park, *Nature (London)* **411**, 665 (2001).
²F. Capasso, J. Faist, and C. Sirtori, *J. Math. Phys.* **37**, 4775 (1996).
³Y. Imry, *Introduction to Mesoscopic Physics* (Oxford Univ. Press, Oxford, 1997).
⁴G. Bergmann, *Phys. Rep.* **107** 1 (1984).
⁵W.J. Skocpol, P.M. Mankiewich, R.E. Howard, L.D. Jackel, D.M. Tennant, and A.D. Stone, *Phys. Rev. Lett.* **56**, 2865 (1986).
⁶S. Washburn and R.A. Webb, *Rep. Prog. Phys.* **55**, 1311 (1992).
⁷N.O. Birge, B. Golding, and W.H. Haemmerle, *Phys. Rev. Lett.* **62**, 195 (1989).
⁸N. Giordano, in *Mesoscopic Phenomena in Solids*, edited by B.L. Altshuler, P.A. Lee, and R.A. Webb (Elsevier, New York, 1991), p. 131.
⁹R.A. Webb, S. Washburn, C.P. Umbach, and R.B. Laibowitz, *Phys. Rev. Lett.* **54**, 2696 (1985).
¹⁰E. Abrahams, P.W. Anderson, P.A. Lee, and T.V. Ramakrishnan, *Phys. Rev. B* **24**, 6783 (1981); H. Fukuyama and E. Abrahams, *ibid.* **27**, 5976 (1983); J.M.B. Lopes dos Santos, *ibid.* **28**, 1189 (1983).
¹¹B.L. Altshuler, A.G. Aronov, and D.E. Khmel'nitsky, *J. Phys. C* **15**, 7367 (1982).
¹²Ya. M. Blanter, *Phys. Rev. B* **54**, 12807 (1996).
¹³A. Stern, Y. Aharonov, and Y. Imry, *Phys. Rev. A* **41**, 3436 (1990).
¹⁴P. Mohanty, E.M.Q. Jariwala, and R.A. Webb, *Phys. Rev. Lett.* **78**, 3366 (1997).
¹⁵F. Pierre and N.O. Birge, *Phys. Rev. Lett.* **89**, 206804 (2002).
¹⁶P. Mohanty and R.A. Webb, *Phys. Rev. Lett.* **91**, 066604 (2003).
¹⁷S. Feng, P.A. Lee, and A.D. Stone, *Phys. Rev. Lett.* **56**, 1960 (1986).
¹⁸P.A. Lee, A.D. Stone, and H. Fukuyama, *Phys. Rev. B* **35**, 1039 (1987).
¹⁹A.D. Stone, *Phys. Rev. B* **39**, 10736 (1989).
²⁰J.S. Moon, N.O. Birge, and B. Golding, *Phys. Rev. B* **56**, 15124 (1997).
²¹P. McConville and N.O. Birge, *Phys. Rev. B* **47**, 16667 (1993).
²²D. Hoadley, P. McConville, and N.O. Birge, *Phys. Rev. B* **60**, 5617 (1999).
²³I.L. Aleiner and Ya. M. Blanter, *Phys. Rev. B* **65**, 115317 (2002).
²⁴I.L. Aleiner, private communication (2003).
²⁵J.J. Lin and N. Giordano, *Phys. Rev. B* **35**, 1071 (1987).
²⁶N.W. Ashcroft and N.D. Mermin, *Solid State Physics* (Holt, Rinehart, and Winston, New York, 1976).
²⁷J.H. Scofield, *Rev. Sci. Instrum.* **58**, 985 (1987).
²⁸F. Pierre, A.B. Gougam, A. Anthore, H. Pothier, D. Esteve, and N.O. Birge, *Phys. Rev. B* **68**, 085413 (2003).
²⁹B.L. Altshuler and A.G. Aronov, in *Electron-electron Interactions in Disordered Systems*, edited by A.L. Efros and M. Pollak (North-Holland, Amsterdam, 1985), p. 1.
³⁰C.W.J. Beenakker and H. van Houten, *Phys. Rev. B* **37**, 6544 (1988).
³¹J. Pelz and J. Clarke, *Phys. Rev. B* **36**, 4479 (1987).
³²S. Hershfield, *Phys. Rev. B* **37**, 8557 (1988).
³³I.L. Aleiner, B.L. Altshuler, and M.E. Gershenson, *Waves Random Media* **9**, 201 (1999).